MBOC PERFORMANCE IN UNAMBIGUOUS ACQUISITION

Md. Farzan Samad and Elena Simona Lohan

Department of Communications Engineering, Tampere University of Technology
P.O.Box 553, FIN-33101, Finland;
{md.samad; elena-simona.lohan}@tut.fi

ABSTRACT

GPS-Galileo Working Group on Interoperability and Compatibility has recommended Multiplexed Binary Offset Carrier (MBOC) modulation in order to increase the tracking abilities of Galileo Open Service signals and of GPS L1 civil signal. MBOC modulation also ensures a better spectral separation with C/A codes. But in the envelope of the Autocorrelation Function (ACF) of MBOC, additional sidelobes appear, which make the acquisition process more challenging. To eliminate the additional sidelobes, unambiguous acquisition techniques have been proposed. The purpose of this paper is to compare different MBOC implementations with sine BOC (SinBOC) performance and also to compare the performance of different types of unambiguous techniques in MBOC modulation.

BIOGRAPHIES

Md. Farzan Samad obtained the B.Sc. degree in Computer Science and IT from Islamic University of Technology (IUT), Bangladesh, in 2004. Currently, he is an M.Sc. student in the Department of Communications Engineering in Tampere University of Technology (TUT), Finland and he is expected to graduate by end of May 2009.

Elena Simona Lohan obtained the M.Sc. degree in Electrical Engineering from the Politehnica University of Bucharest, Romania, in 1997, the D.E.A. degree in Econometrics, at Ecole Polytechnique, Paris, France, in 1998, and the Ph.D. degree in Telecommunications from Tampere University of Technology. In 2007 she was nominated as a Docent in the field of "Wireless communication techniques for personal navigation". Since November 2003, Simona Lohan has been working as a Senior Researcher at TUT and she has been acting as a group leader for the mobile and satellite-based positioning activities at the Department of Communications Engineering. Her research interests include satellite positioning techniques, CDMA signal processing, and wireless channel modelling and estimation. She was also involved with the EU FP6 project GREAT.

I. INTRODUCTION

MBOC modulated signals are the main candidates for the future Galileo Open Services (OS) and GPS L1C signals [1]. The power spectral density (PSD) of MBOC is a combination of SinBOC(1,1) and SinBOC(6,1) spectra. The SinBOC(6,1) sub-carrier increases the power on the higher frequencies, which results in signals with narrower main lobe of the correlation function envelope and better receiver level performance [2]. The narrower main lobe allows a better accuracy in the delay tracking process. In contrary, additional sidelobes appear in the ± 1 chip interval of the Absolute value of the Autocorrelation Function (AACF) of MBOC [3]. These additional sidelobes make the AACF ambiguous which complicates the acquisition process. One way to overcome this problem is to reduce the step of searching the time bins, which increases the acquisition time. In order to avoid the ambiguities of the AACF and also to keep the step of the time bin sufficiently high (e.g., half of the width of the main lobe in AACF), unambiguous acquisition techniques have been proposed in [4], [5], [6], [7], [3], [8]. These unambiguous acquisition techniques are denoted as: Betz and Fishman (B&F), Martin and Heiries (M&H) and Unsuppressed Adjacent Lobes (UAL) methods, respectively. A detailed description of those and their comparison in SinBOC(1,1) case can be found in [8].

The purpose of this paper is two-fold: first, to compare the performance of SinBOC(1,1) with different MBOC implementations, and second, to analyze the performance of ambiguous MBOC (aMBOC) and of different types of unambiguous ('BPSK like') MBOC acquisition techniques. The analysis of unambiguous methods in the context of MBOC signal acquisition is completely new, to the extent of the authors' knowledge.

II. SIGNAL MODEL

MBOC modulation places small amount of code power at higher frequencies, which improves the code tracking performance [1], [9], [10]. The Power Spectral Density (PSD) of MBOC(6,1,1/11) is a combination of SinBOC(1,1) spectrum and SinBOC(6,1) spectrum. It is possible to use a number of different time waveforms to generate MBOC(6,1,1/11) spectrum, which gives implementation flexibility. According to GJU recommendation [1], PSD for MBOC was fixed to:

$$G_{MBOC}(f) = \frac{10}{11} G_{SinBOC(1,1)}(f) + \frac{1}{11} G_{SinBOC(6,1)}(f), \quad (1)$$

where $G_{SinBOC(m,n)}(f)$ is the normalized PSD of SinBOC(m,n)-modulated PRN code, given by [11], [12]:

$$G_{SinBOC(m,n)}(f) = \frac{1}{T_c} \left(\frac{sin(\pi f \frac{T_c}{N_B}) sin(\pi f T_c)}{\pi f cos(\pi f \frac{T_c}{N_B})} \right)^2 \quad (2)$$

In the above equation, $m = f_{sc}/f_{ref}$ and $n = f_c/f_{ref}$, where f_{sc} is the sub-carrier frequency, f_c is the chip frequency and $f_{ref} = 1.023$ MHz is the reference C/A code frequency [11]. $N_B = 2f_{sc}/f_c = 2m/n$ is the BOC modulation index.

The PSD of MBOC and SinBOC(1,1) signals are shown in Figure 1. The PSD of MBOC of eqn.(1) is the total PSD of pilot and data signals together. Due to SinBOC(6,1) component, extra peaks can be noticed at around ± 6 MHz of the MBOC PSD as compared to SinBOC(1,1) case. Several implementations of MBOC exists, and the two main ones are: the Composite BOC (CBOC) and the Time Multiplexed BOC (TMBOC), described in what follows. The CBOC method is based on a weighted sum (or difference) of SinBOC(1,1) and SinBOC(6,1)-modulated code symbols [12]. Following the BOC

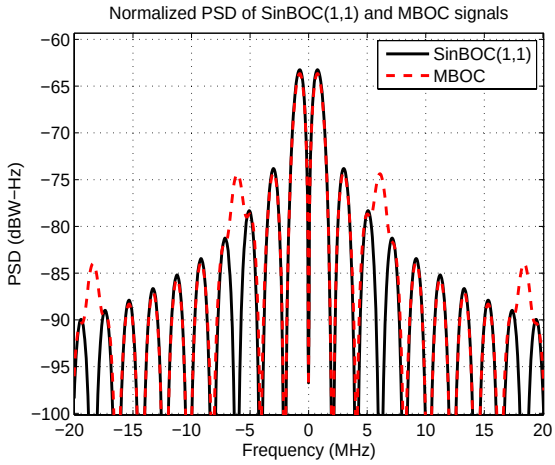

Fig. 1. PSD for MBOC and SinBOC(1,1)-modulated signals.

model and derivations of [12], the composite sum or difference can be written as:

$$\begin{aligned} s_{CBOC}(t) &= w_1 s_{SinBOC(1,1),held}(t) \\ &+ w_2 s_{SinBOC(6,1)}(t) \\ &= w_1 \sum_{i=0}^{N_{B_1}-1} \sum_{k=0}^{\frac{N_{B_2}}{N_{B_1}}-1} (-1)^i c\left(t - i\frac{T_c}{N_{B_1}} - k\frac{T_c}{N_{B_2}}\right) \\ &+ w_2 \sum_{i=0}^{N_{B_2}-1} (-1)^i c\left(t - i\frac{T_c}{N_{B_2}}\right) \end{aligned} \quad (3)$$

where $s_{SinBOC(1,1),held}$ is the SinBOC(1,1)-modulated signal, held at the same rate with $s_{SinBOC(6,1)}$, the SinBOC(6,1)-modulated signal, $N_{B_1} = 2$ is the BOC modulation order for SinBOC(1,1) signal, $N_{B_2} = 12$ is the BOC modulation order for SinBOC(6,1) signal, and w_1 and w_2 are some (positive or negative) weighting factors such that ${w_1}^2 + {w_2}^2 = 1$. There are 3 proposed implementations of CBOC: CBOC('+') $(w_1, w2 > 0)$, CBOC('-') $(w_1 > 0,\ w2 < 0)$ and CBOC('+/-') which is a combination of the 2 previous ones: we use CBOC('+') for even chips and CBOC('-') for odd chips [10]. The results of this paper used CBOC('+') among the CBOC implementations and TMBOC. We remark that the CBOC('+') is the modulation proposed for E1 data

channels in the last Galileo SIS-ICD specification document [13].

In eq. 3, $c(t)$ is the pseudorandom code:

$$c(t) = \sqrt{E_b} \sum_{n=-\infty}^{\infty} b_n \sum_{m=1}^{S_F} c_{m,n} p_{T_{B_2}}(t - nT_c S_F - mT_c), \quad (4)$$

where b_n is the n-th code symbol, E_b is the code symbol energy, $S_F = 1023$ chips is the spreading factor or number of chips per code symbol, $c_{m,n}$ is the m-th chip corresponding to the n-th symbol, T_c is the chip rate, and $p_{T_{B_2}}(\cdot)$ is a rectangular pulse of support T_c/N_{B_2} and unit amplitude.

In TMBOC implementation, the whole signal is divided into blocks of N code symbols and $M < N$ of N code symbols are SinBOC(1,1)-modulated, while $N - M$ code symbols are SinBOC(6,1)-modulated [12]. Using derivations from [12], TMBOC waveforms can be written as:

$$\begin{aligned} s_{TMBOC}(t) &= \sqrt{E_b} \sum_{n \in \mathcal{S}} b_n \sum_{m=1}^{S_F} c_{m,n} \sum_{i=0}^{N_{B_1}-1} \sum_{k=0}^{\frac{N_{B_2}}{N_{B_1}}-1} (-1)^i p_{T_{B_2}}(t - i\frac{T_c}{N_{B_1}} - k\frac{T_c}{N_{B_2}}) \\ &+ \sqrt{E_b} \sum_{n \notin \mathcal{S}} b_n \sum_{m=1}^{S_F} c_{m,n} \sum_{i=0}^{N_{B_2}-1} (-1)^i p_{T_{B_2}}(t - i\frac{T_c}{N_{B_2}}) \end{aligned} \quad (5)$$

where $\mathcal{S}$ is the set of chips (or spreading symbols) which are SinBOC(1,1) modulated (i.e., if I is the total set of symbols, then card(S)/card(I) = M/N, where card$(\cdot)$ stands for the cardinality of a set).

Based on eqns.(3) and (5) and using the facts that $M, N << \infty$ and that, since $|w_1|, |w_2|$ are amplitude coefficients, $|\cdot|$ is the absolute value operator, and $M, N - M$ define the power division between SinBOC(1,1) and SinBOC(6,1), the following relationship can be set between $|w_1|, |w_2|$ and M, N: $|w_1| = \sqrt{\frac{M}{N}}$ and $|w_2| = \sqrt{\frac{N-M}{N}}$. Therefore, according to [12], the unified CBOC/TMBOC model can be written as:

$$\begin{aligned} s_{MBOC}(t) &= w_1 c_\delta(t) \circledast s_1(t) \circledast p_{T_{B_2}}(t) \\ &+ w_2 c_\delta(t) \circledast s_2(t) \circledast p_{T_{B_2}}(t) \end{aligned} \quad (6)$$

where $\delta(\cdot)$ is the Dirac pulse, $\circledast$ is the convolution operator, $c_\delta(t)$ is the code signal without pulse shaping:

$$c_\delta(t) = \sqrt{E_b} \sum_{n=-\infty}^{\infty} b_n \sum_{m=1}^{S_F} c_{m,n} \delta(t - nT_c S_F - mT_c), \quad (7)$$

and $s_1(t)$, $s_2(t)$ are SinBOC-modulated parts (with associated hold block when needed), given by:

$$s_1(t) = \sum_{i=0}^{N_{B_1}-1} \sum_{k=0}^{\frac{N_{B_2}}{N_{B_1}}-1} (-1)^i \delta(t - i\frac{T_c}{N_{B_1}} - k\frac{T_c}{N_{B_2}}), \quad (8)$$

and, respectively:

$$s_2(t) = \sum_{i=0}^{N_{B_2}-1} (-1)^i \delta(t - i\frac{T_c}{N_{B_2}}) \quad (9)$$

An example of CBOC('+') and TMBOC modulated waveforms, together with the PRN sequence before modulation is shown in Fig. 2. For comparison purposes, also CBOC('-') and CBOC('+/-') modulated signals are shown in Fig. 3, for the same PRN code as in Fig. 2.

III. UNAMBIGUOUS ALGORITHMS

Betz & al. [7], [14] and Fishman & al. [6] proposed single and dual Side-Band (SB) acquisition methods which are denoted here as B&F methods, after the initials of the main authors. The main idea behind B&F algorithm applied to MBOC case is to select only the main lobes of the MBOC modulated received signal and of the reference code, respectively and to filter out the side bands. The Single-SB (SSB) B&F method considers either upper or lower band during constructing the decision statistic. Single-SB B&F method requires one complex SB-selection filter for the real code and two complex SB-selection filters for the received signal. On the other hand, the required number of filters for Dual-SB (DSB) B&F method is twice than that of single-SB. The reference code is the MBOC-modulated code sequence. The

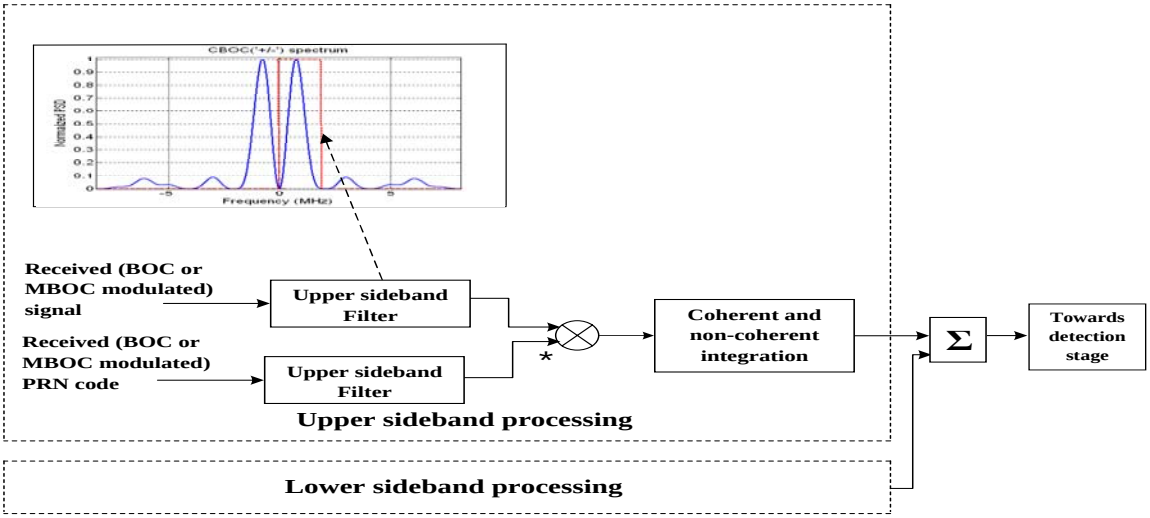

Fig. 4. B&F principle in MBOC acquisition.

non-coherent correlation loss is higher in single-SB method comparing to dual-SB method [3], [6], [8]. The block diagram of B&F method is illustrated in Fig. 4 for MBOC spectrum.

BPSK-like techniques were initially proposed by Martin & al. [4] and by Heiries & al. [5], and denoted in what follows by M&H methods. Both principal lobes and all secondary lobes between the 2 main lobes are selected for the correlation purpose in M&H algorithm. The main difference compared with B&F method is the fact that only one filter is required (thus, ensuring a lower complexity solution). A modification to the original M&H algorithm of [5] was proposed in [15], [16], [8] and this is the approach used here (still referred to as M&H for simplicity sake). Its block diagram is illustrated in Fig. 5. The $\widehat{a}$ factor is a modulation-dependent factor, as shown in [8]. For MBOC cases considered in this paper, $\widehat{a} = 1$. In M&H, the number of required filters for single-SB and dual-SB methods is the same. Also the reference code is not the filtered BOC-modulated code, but the BPSK-modulated code sequence, held at the same rate as MBOC signal.

In Unsuppressed Adjacent Lobes (UAL) method, the filter part is completely removed [8], which reduces the complexity of the receiver part even more. As the lobes which are adjacent to the main lobes are unsuppressed, this may affect the performance of the acquisition block. As for M&H case, the reference code is BPSK modulated code sequence of ± 1, held at MBOC rate. The UAL block diagram is similar with the M&H block diagram of Fig. 5, with the only difference that the 'low-pass filters' in upper and lower sidebands are completely removed.

The 3 above-mentioned unambiguous algorithms are described in detail in [8]; the modifications for MBOC signal are rather straightforward by taking into account the MBOC signal characteristics, as explained in Section II.

In Fig. 6, the normalized AACFs for aMBOC and the non ambiguous MBOC (TMBOC implementation) algorithms are shown. Similar plots are obtained for the other MBOC implementations. Clearly, the ambiguities of the AACF disappears after unambiguous processing.

IV. SIMULATION RESULTS

Simulations were carried out in single path scenario for MBOC-modulated signals and static channel model was considered, in order to find out the maximum achievable performance of unambiguous algorithms for MBOC. Serial single-dwell search strategy was employed. The algorithms used for the simulations are: ambiguous MBOC from [2], [8] and the 3 unambiguous methods described in Section III: B&F, UAL, and M&H. For the single-sideband (SSB) correlation methods, only the positive band is used; for the dual-sideband correlation (DSB) methods both

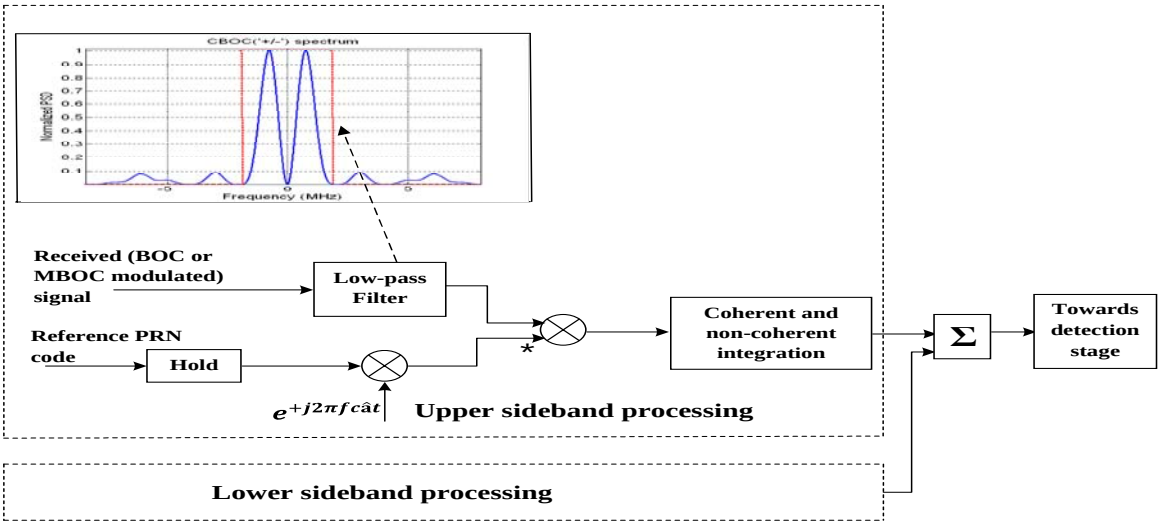

Fig. 5. M&H principle in MBOC acquisition.

positive and negative bands are used and combined non-coherently. The oversampling factor N_s for the received signal was 4 samples per MBOC interval (one MBOC interval has $1/12$ chips length), and the time-bin step $(\Delta t)_{bin}$ was half of the width of the main lobe (i.e., 0.35 chips). A coherent integration time, $N_c = 20$ ms was used, followed by non-coherent integration on N_{nc} blocks (here, $N_{nc} = 1$) .

Fig. 7 compares the performance of unambiguous methods with various MBOC implementations, namely: TMBOC, CBOC('+') with $W_1 = w_1^2 = 10/11$ and $W_2 = w_2^2 = 1/11$ and CBOC('+') with $W_1 = 29/33$ and $W_2 = 4/33$. Also SinBOC(1,1) is shown as reference. DSB acquisition was used here. From the results, we can observe, as expected, that SinBOC(1,1) is giving better detection probability (P_d) values than MBOC implementations but the performance deterioration of MBOC is not significant. And among different MBOC implementations, CBOC('+') results are slightly better than TMBOC, and the weights choice in CBOC('+') implementation has very little impact on the acquisition performance.

Further on, time-domain based correlation was compared with FFT-based (frequency domain-based) correlations in Fig. 8. Similar results were obtained for CBOC; here only TMBOC is shown for convenience. The statistics were computed for $N_{rand} = 1000$ random realizations for each particular CNR. The CNR values are plotted in dB-Hz. In the acquisition stage, one important parameter is $(\Delta t)_{bin}$, which is generally half of the width of the main lobe, but smaller steps may be used for getting better P_d values (with the tradeoff of longer acquisition times). In Fig. 8, we also compared the unambiguous methods with the ambiguous MBOC acquisition. Clearly, DSB unambiguous acquisition outperforms the ambiguous acquisition, while SSB unambiguous acquisition is still better than ambiguous acquisition at sufficiently high CNRs. Some examples of achievable P_d at $CNR = 30$ dB-Hz are: $P_d = 0.88$ for B&F DSB case, $P_d = 0.71$ for M&H DSB case, $P_d = 0.7$ for UAL DSB case, and $P_d = 0.44$ for aMBOC, which is quite low comparing to non ambiguous algorithms. And among non ambiguous methods, B&F is giving better P_d values than UAL and M&H methods, as noticed before [8] for SinBOC(1,1) cases only. It is seen that time-domain correlations give slightly better results than FFT-domain correlations but the performance difference is marginal. On the other hand, time-domain correlations take longer time to execute than FFT-domain correlations. Therefore, further on FFT-domain correlations are considered.

The effect of the time-bin step $(\Delta t)_{bin}$ is shown in Fig. 9 for TMBOC with unambiguous DSB methods at 25 dB-Hz (similar results were obtained for CBOC implementations). False alarm probability was P_{fa}=10^{-3} and $(\Delta t)_{bin} = 0.0208$ till 1 chip were

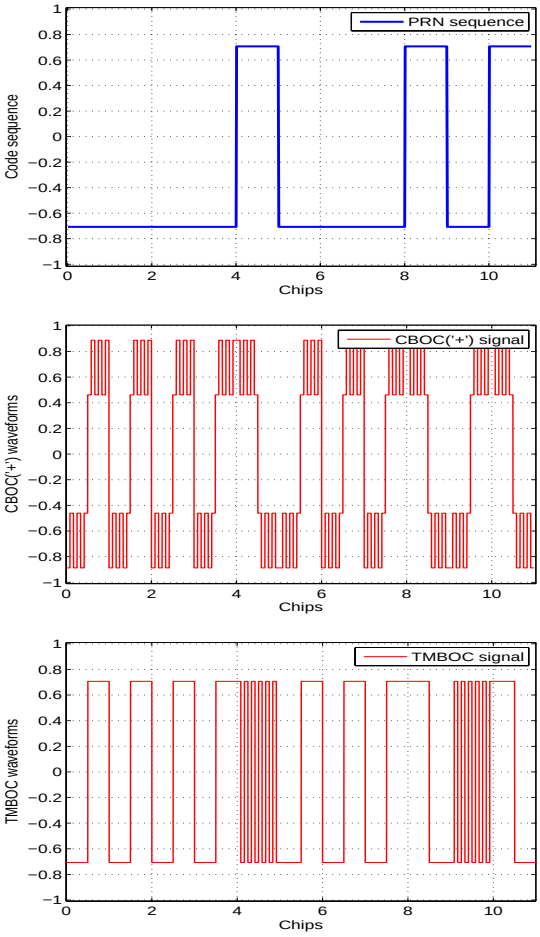

Fig. 2. A snapshot of PRN sequence (upper plot) and of CBOC('+') (middle plot) and TMBOC (lower plot)-modulated signals.

considered. Clearly, as the step increases, the detection probability decreases, but the unambiguous DSB methods outperform the aMBOC even at low steps. B&F unambiguous method performs the best.

In Fig. 10, the Region of Convergence (ROC) performance is compared for different algorithms. Here, $CNR = 30$ dB-Hz and P_{fa} range was 10^{-5} to 10^{-1}. We observe that the unambiguous MBOC algorithms outperforms the aMBOC also at different P_{fa} levels. For example, at $P_{fa} = 2 * 10^{-2}$, the P_d values are 0.71, 0.99, 0.93 and 0.94 for aMBOC, B&F, UAL and M&H, respectively.

The effect of the oversampling factor (P_d vs N_s) for TMBOC DSB unambiguous acquisition is shown in Fig. 11. N_s range was between 1 and 7. From

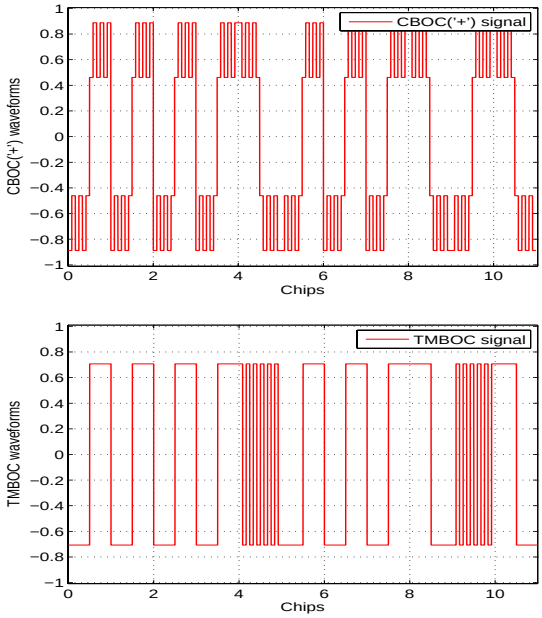

Fig. 3. A snapshot of CBOC('-') (upper plot) and CBOC('+/-') (lower plot)-modulated signals.

Fig. 11 we observe that P_d remains invariant over N_s, as expected. Therefore, minimum N_s can be safely chosen for simulations (in order to decrease the simulation time).

Fig. 12 shows the effect of coherent integration (P_d vs. N_c), at $CNR = 25$ dB-Hz. We observe that P_d increases with the increase of coherent integration time, as expected, and also that the increase of P_d of B&F is much higher than other methods.

Fig. 13 shows the impact of a residual frequency error in the acquisition outputs, i.e., when the frequency bin center in the correct bin is not centered at 0, but at a $(\Delta f)_{err}$. Here, $N_c = 20$ ms, therefore the frequency bin size was $1000/2/N_c = 25$ Hz. Clearly, after 25 Hz residual frequency error, the P_d is highly degraded.

The impact of the power percentage per pilot channel in MBOC modulation is shown in Fig. 14. Here, X_{power} denotes the power percentage of pilot channel. Based on the value of X_{power}, the weights for BOC(1,1) and BOC(6,1) modulations are set. For example, when $X_{power} = 0.5$ then based on calculation, the squared weights are $W_1 = 9/11$ and $W_2 = 2/11$ for SinBOC(1,) and SinBOC(6,1), respectively. In Fig. 14, X_{power}=[0.25 0.5 0.75 1]

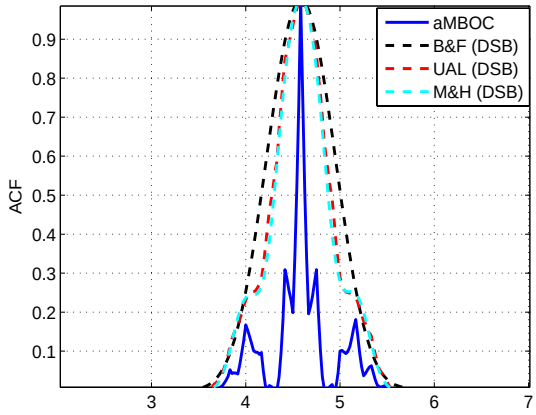

Fig. 6. Normalized AACFs for TMBOC for DSB correlation methods

and $CNR = 30$ dB-Hz. Clearly, more power we have on pilot channel, then more weight is put on SinBOC(1,1) component, and better is the acquisition performance.

V. CONCLUSIONS

MBOC modulation has been proposed for future satellite signals in order to enhance the delay tracking in multipath scenario. However, the acquisition performance with MBOC is deteriorated compared to SinBOC(1,1) case, as shown here. Additionally, in this paper, the performance of the unambiguous acquisition methods was thoroughly studied with various MBOC implementations. Results were also compared with SinBOC(1,1) case. It was shown that unambiguous acquisition algorithms, previously proposed for SinBOC(1,1) are working well also for MBOC modulation. It was also shown that there performance deterioration in the acquisition stage of MBOC compared with SinBOC(1,1) modulation is rather small, especially when Betz&Fishman dual-side-band acquisition method is employed. The impact of various receiver parameters (time-bin step, residual Doppler error, coherent integration time, oversampling factor, and desired false alarm probability) on the detection probability in the acquisition stage was also shown here.

ACKNOWLEDGMENT

This work was carried out in the project "Future GNSS Applications and Techniques (FUGAT)" funded by the Finnish Funding Agency for Technology and Innovation (Tekes). This work has also been supported by the Academy of Finland.

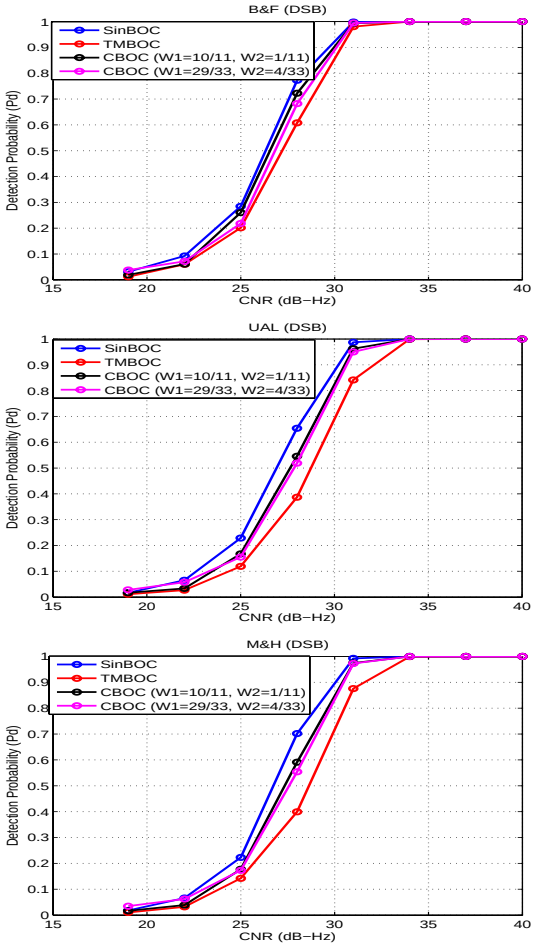

Fig. 7. Performance comparison of unambiguous acquisition (from top till bottom: B&F, UAL, and M&H) for different BOC implementations. SinBOC(1,1) is also shown as reference.

VI. REFERENCES

[1] "Galileo joint undertaking - GPS-Galileo Working Group A (WGA) Recommendations on L1 OS/LIC optimization ," March 2006.

[2] F. Dovis, L. Presti, M. Fantino, P. Mulassano, and J. Godet, "Comparison between Galileo CBOC Candidates and BOC(1,1) in Terms of Detection Performance," in *International Journal of Navigation and Observation*, 2008.

[3] E. Lohan, "Statistical analysis of BPSK-like techniques for the acquisition of Galileo sig-

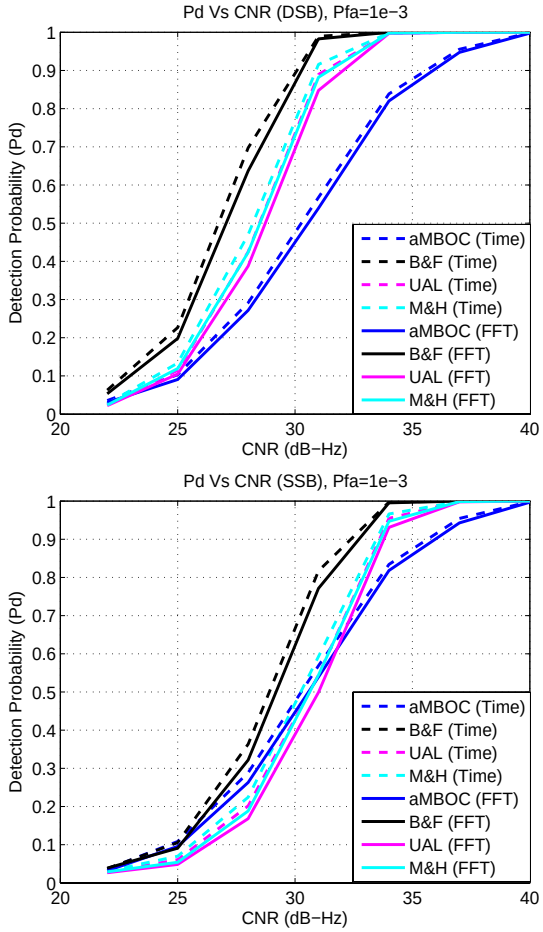

Fig. 8. P_d vs. CNR for TMBOC in Time and FFT domains for DSB methods (up), SSB methods (down)

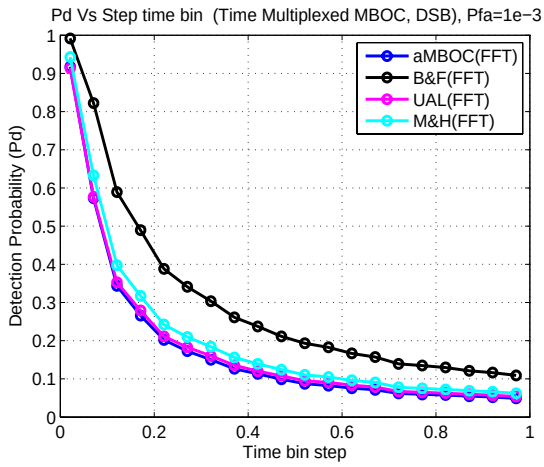

Fig. 9. P_d vs $(\Delta t)_{bin}$ for TMBOC in FFT domain for DSB methods for CNR=25 dB-Hz

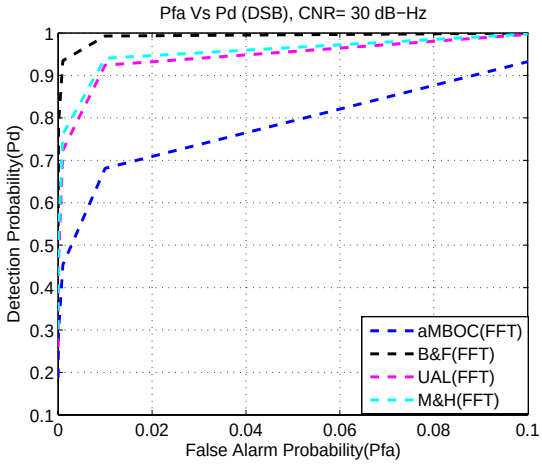

Fig. 10. P_d vs. P_{fa} for TMBOC in FFT domain for DSB methods

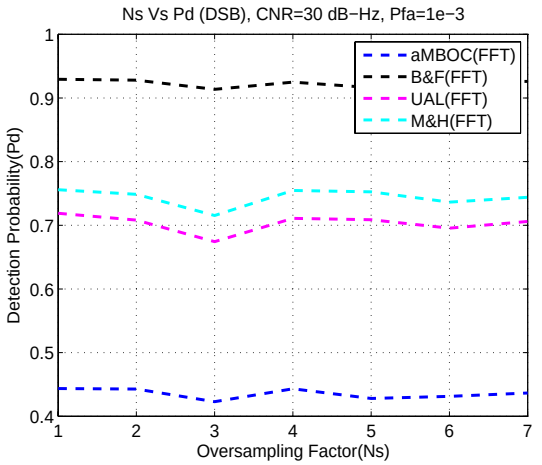

Fig. 11. P_d vs. N_s for TMBOC in FFT domain for DSB unambiguous methods

nals," *AIAA Journal of Aerospace Computing, Information, and Communication*, vol. 3, pp. 234–243, May 2006.

[4] N. Martin, V. Leblond, G. Guillotel, and V. Heiries, "BOC (x,y) signal acquisition techniques and performances," in *ION-GPS2003*, (Portland, OR, US), Septempber 2003.

[5] V. Heiries, D. Oviras, L. Ries, and V. Calmettes, "Analysis of non ambiguous BOC signal acquisition performances," in *ION-GNSS*, (Long Beach, CA, US), Septempber 2004.

[6] P. Fishman and J. Betz, "Predicting performances of direct acquisition for the M-code

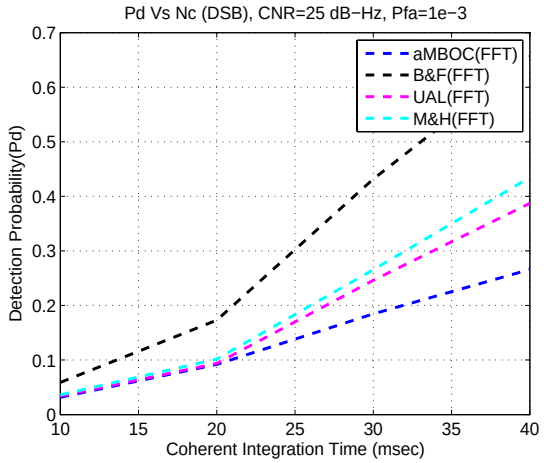

Fig. 12. P_d vs. N_c for TMBOC in FFT domain for DSB unambiguous methods

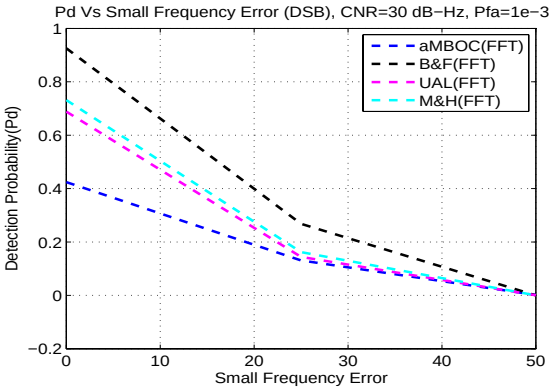

Fig. 13. P_d vs. Small Frequency Error $(\Delta f)_{err}$) for TMBOC and DSB unambiguous methods

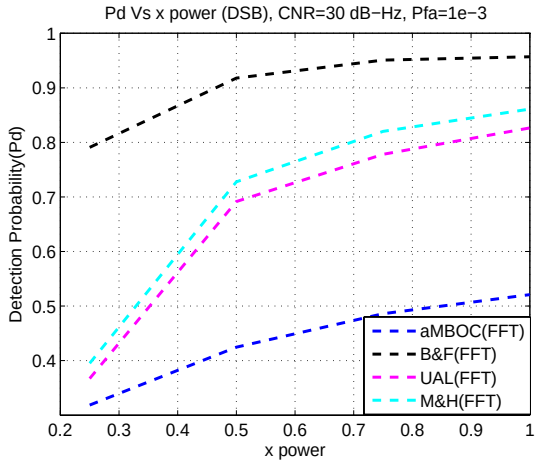

Fig. 14. P_d vs. X_{power} for TMBOC

signal," in *ION-NMT*, 2000.

[7] J. Betz and P. Capozza, "System for direct acquisition of received signals," in *US Patent Application Publication*, (US), April 2004.

[8] E. Lohan, A. Burian, and M. Renfors, "Low-complexity acquisition methods for split-spectrum CDMA signals," *Wiley International Journal of Satellite Communications*, 2008.

[9] G. Hein, J. Avila-Rodriguez, S. Wallner, J. Betz, C. Hegarty, J. Rushanan, A. Kraay, A. Pratt, S. Lenahan, J. Owen, J. Issler, and T. Stansell, "MBOC: The New Optimized SpreadingModulation Recommended for GALILEO L1 OS and GPS L1C," in *Inside GNSS - Working Papers, no. 4 in 1, pp. 5765*, 2006.

[10] J. Avila-Rodriguez, S. Wallner, G. Hein, E. Rebeyrol, O. Julien, C. Macabiau, L. Ries, A. De-Latour, L. Lestarquit, and J. Issler, "CBOC - An Implementation of MBOC," in *First CNES Workshop on Galileo Signals and Signal Processing*, (Toulouse, France), October 2006.

[11] J. W. Betz, "The Offset Carrier Modulation for GPS modernization," in *Proc. of ION Technical meeting, pp. 639648,*, 1999.

[12] E. Lohan and M. Renfors, "Correlation properties of Multiplexed-BOC (MBOC) modulation for future GNSS signals," in *European Wireless Conference*, (Paris, France), April 2007.

[13] "Galileo open service signal in space interface control document os sis icd, draft 1." European Space Agency and European GNSS Supervisory Authority, Specifications Document, Feb 2008.

[14] B. Barker, J. Betz, J. Clark, J. Correia, J. Gillis, S. Lazar, K. Rehborn, and J. Straton, "Overview of the GPS M Code Signal," in *CDROM Proc. of NMT*, 2000.

[15] A. Burian, E. Lohan, and M. Renfors, "BPSK-like Methods for Hybrid- Search Acquisition of Galileo Signals," in *IEEE International Conference on Communications (ICC 2006)*, (Istanbul, Turkey), p. 52115216, Jun 2006.

[16] A. Burian, E. Lohan, V. Lehtinen, and M. Renfors, "Complexity Considerations for Unambiguous Acquisition of Galileo Signals," in *3rd Workshop on Positioning, Navigation and Communication 2006 (WPNC 2006)*, (Hannover, Germany), pp. 65–73, Mar 2006.